Tumour-Purity Adjustment of Published Prognostic Transcriptomic Signatures: A Pan-Cancer Audit in 12 TCGA Cohorts

Tianjiao Wang
Wenzhou-Kean University
Computer Science, The College of Science, Mathematics and Technology
Wenzhou, China
wantianj@kean.edu

Abstract

Prognostic transcriptomic signatures are commonly evaluated in bulk tumour tissue, where measured expression reflects malignant cells together with stromal and immune compartments. Tumour purity may therefore be associated with both a signature score and survival, complicating the interpretation of an unadjusted prognostic coefficient. We conducted a pan-cancer audit of published prognostic transcriptomic signatures across 12 The Cancer Genome Atlas (TCGA) cohorts, examining how purity adjustment changes their associations with overall survival. The inventory comprised 54 eligible published signatures, six reference gene sets, and two additional published signatures excluded for insufficient gene coverage. One included ovarian lncRNA signature could not be scored in its intended cohort because a component gene had zero variance, yielding 53 published signatures and six reference sets (59 distinct scored sets) across 129 signature–cohort pairs. The primary analysis included 5,417 patients and 1,939 deaths. After false-discovery-rate correction, 97 of 129 pairs showed an association between signature score and ABSOLUTE purity. The median absolute coefficient change after purity adjustment was 0.022; four pairs were classified as attenuated, 13 as amplified, and 112 as not distinguishable from zero. All four attenuated pairs were reference sets rather than published prognostic signatures. The magnitude and classification of coefficient changes varied across purity estimators, highlighting the importance of estimator choice when evaluating prognostic transcriptomic signatures. These findings describe conditional associations and do not imply a causal effect of tumour purity.

CCS Concepts

• **Applied computing** → **Bioinformatics**; *Life and medical sciences*; • **Mathematics of computing** → *Survival analysis*; *Regression analysis.*

Keywords

tumour purity, prognostic gene-expression signatures, TCGA, Cox regression, tumour microenvironment, survival analysis, reproducibility

1 Introduction

Gene-expression signatures are widely used to summarise tumour biology and stratify patients by prognosis. Many such signatures are developed from bulk tumour transcriptomes and are subsequently interpreted as measurements of malignant-cell programmes. Bulk expression, however, is a mixture: the observed profile reflects malignant cells, immune infiltrates, fibroblasts, vascular cells, and other non-malignant components. The relative abundance of these compartments varies across samples and cancer types. A signature can therefore capture a combination of tumour-cell-intrinsic biology and microenvironmental composition, even when its original biological interpretation is narrower.

Tumour purity provides one summary of this mixture. DNA-based approaches such as ABSOLUTE estimate the fraction of malignant cells from somatic copy-number information, while expression-based approaches such as ESTIMATE infer tumour purity and stromal or immune admixture from transcriptomic profiles. Other tools estimate cellular fractions through deconvolution. These approaches do not measure exactly the same construct and can disagree across cohorts and methods [1–3, 9, 72, 75, 81, 101]. Pan-cancer studies have characterised the immune landscape of tumours and related immune and stromal estimates to clinical outcomes and mutation profiles [6, 34, 43, 86]. The resulting estimates are useful, but they are not interchangeable measurements of a single error-free quantity.

The prognostic relevance of the tumour microenvironment is well established. Stromal expression has been associated with outcome in breast, colorectal, and pancreatic cancers, and fibroblast-related programmes can dominate scores that were intended to represent cancer-cell-intrinsic properties [8, 25, 31, 53, 56, 70, 71]. Immune and stromal signals may themselves be biologically meaningful rather than mere nuisance variation. Conversely, a signature derived from bulk expression may partly reflect the abundance of non-malignant cells, and its apparent prognostic association may change after adjustment for purity. The distinction is important because the coefficient of a signature in a multivariable survival model is not a direct measure of biological causation.

Published prognostic signatures also vary in their derivation cohorts, scoring rules, gene coverage, and validation strategies. Random gene sets can show apparent associations with outcome, and different signatures can yield similar predictions despite limited gene overlap. Proliferation-related genes can account for substantial prognostic signal, while test-set bias and incomplete external validation can limit reproducibility [20, 26, 28, 39, 73, 80, 85, 88, 92]. More recent work has compared hypoxia signatures and transcriptomic tumour-infiltrating-lymphocyte signatures across cancers [24, 42]. A recent preprint benchmarks published triple-negative breast-cancer signatures, an external-validation study examines prognostic signatures in head and neck cancer, and a pan-cancer stromal activity score illustrates the intended prognostic use of

microenvironmental measures [23, 32, 82]. These observations motivate a systematic comparison in which signature scoring, cohort membership, and purity adjustment are made explicit.

We conducted a pan-cancer audit across 12 TCGA cohorts to examine whether the association between published prognostic transcriptomic signatures and overall survival changes when tumour purity is added to the Cox model, whether these changes exceed those observed for expression-matched random gene sets, and whether conclusions depend on the purity estimator, scoring method, cohort, or signature category. The estimand is associational: a movement of a coefficient towards zero after adding purity does not establish that purity is a confounder or that a signature is biologically invalid. Adjustment may remove confounding, block a pathway, or alter a conditional hazard ratio for mathematical reasons unrelated to confounding [37, 41, 77, 91].

2 Background and Related Work

2.1 Purity estimation and bulk-expression mixtures

ABSOLUTE estimates tumour purity from allele-specific copy-number data and was used as the primary estimator in this study [9]. Expression-derived approaches include ESTIMATE, which infers stromal and immune components from gene-expression signatures [101], and methods such as xCell that estimate the abundance of multiple cell types [1]. Comparative evaluations of deconvolution methods have shown that estimates depend on the method and the reference profiles used [3, 81]. A purity measure derived from the same expression matrix as a signature also raises a circularity concern: the signature and purity score may share genes by construction. ABSOLUTE avoids this particular source of direct gene overlap, although it remains subject to measurement error and quality-control decisions.

2.2 Microenvironmental signal in prognostic signatures

Stromal gene-expression programmes predict outcome in several tumour types [8, 31, 70]; immune infiltration and cell-type composition are likewise associated with prognosis across cancers [33, 34, 43, 86]. Tumour-associated fibroblasts and immune populations can contribute strongly to bulk expression, while cancer-cell-specific signature construction has been proposed to reduce this dependence [25, 53, 56, 71, 76]. Purity-associated genes have also been proposed as prognostic markers in glioma, hepatocellular carcinoma, and diffuse large B-cell lymphoma [67, 100, 105, 113]. In this study, purity is treated as a covariate for examining how the association of other signatures with survival changes, not as a causal exposure.

2.3 Signature evaluation and statistical interpretation

Random gene sets can be associated with survival even when they lack a coherent biological interpretation [88]. Published signatures may overlap little yet show similar prognostic performance, and repeated evaluation on development data can produce optimistic estimates [28, 39, 73]. Reviews of prognostic microarray studies have emphasised the need for careful validation and transparent reporting [26, 69, 85]. The present audit follows the reporting logic of REMARK, with STROBE and selected TRIPOD+AI items as complementary checks [18, 68, 89]. The interpretation of adjusted coefficients is informed by work on confounding, overadjustment, hazard-ratio non-collapsibility, and the interpretation of coefficients in multivariable models [37, 41, 77, 91].

3 Materials and Methods

3.1 Study design and reporting framework

We conducted an observational, retrospective evaluation of published prognostic gene-expression signatures in public TCGA cohorts. The primary analysis (C1) used ABSOLUTE purity. Four sensitivity settings varied the purity estimator, scoring procedure, or clinical covariate set. The analysis was specified before outcome modelling and followed the REMARK reporting framework, supplemented by STROBE and selected TRIPOD+AI items [18, 68, 89]. Figure 1 summarises the study design.

3.2 Data sources, cohorts, and patient selection

Overall-survival data were obtained from the TCGA Pan-Cancer Clinical Data Resource [64], RNA-sequencing expression from the UCSC Xena Genomic Data Commons hub [35, 38], and ABSOLUTE purity calls from the Pan-Cancer Atlas resource [9]. Expression values are described as $\log_2(\text{TPM}+1)$ with GENCODE v36 annotation. Patient records were linked across sources using the first 12 characters of the TCGA barcode. Consensus purity estimates attributed to Aran and colleagues and ESTIMATE purity values were used in sensitivity analyses [2, 101].

Twelve cohorts were included: lung adenocarcinoma (LUAD), lung squamous cell carcinoma (LUSC), head and neck squamous cell carcinoma (HNSC), kidney renal clear cell carcinoma (KIRC), bladder urothelial carcinoma (BLCA), liver hepatocellular carcinoma (LIHC), breast invasive carcinoma (BRCA), stomach adenocarcinoma (STAD), skin cutaneous melanoma (SKCM), ovarian serous cystadenocarcinoma (OV), lower-grade glioma (LGG), and glioblastoma (GBM). A patient entered a signature–cohort analysis set when overall-survival time and status, RNA-sequencing expression, ABSOLUTE purity, and the covariates retained for that cohort were available.

The twelve cohorts comprised 6,588 TCGA-CDR records; 6,488 had eligible overall-survival information, 5,642 had expression, ABSOLUTE purity, and survival time, and 5,417 complete cases entered the primary analysis, including 1,939 deaths. Figure 2 presents the patient-selection flow and cohort-level record counts. Cohort characteristics are summarised in Table 1. Follow-up is described as a reverse Kaplan–Meier estimate. Stage is not available for OV, LGG, and GBM. Sex is omitted from BRCA and OV models because one sex contributed fewer than ten events in each cohort.

3.3 Gene-set inventory and scoring

The inventory comprised group A (published, cancer-specific prognostic signatures) and group B (reference gene sets). Group-A signatures were applied only to the cancer type or types for which they were developed; glioma signatures were applied in both LGG and GBM. The inventory included 54 group-A signatures and six

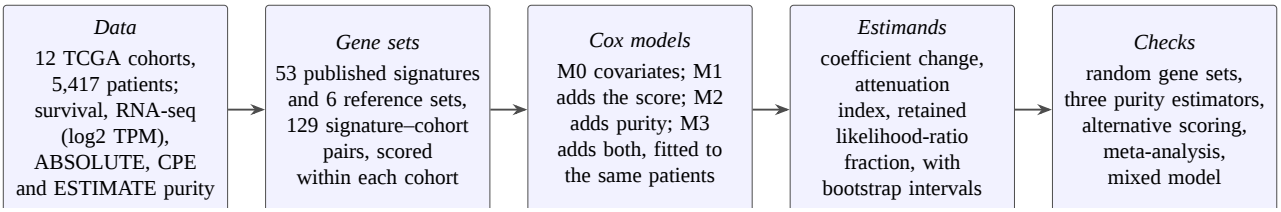
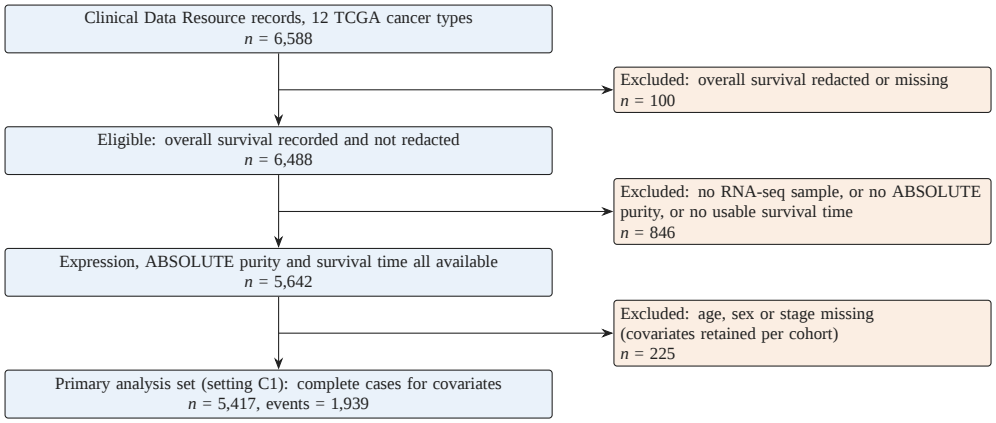


Figure 1: Study workflow. Twelve TCGA cohorts provide survival, expression, and purity data. Fifty-three published signatures and six reference sets are scored across 129 signature–cohort pairs. Four nested Cox models estimate the change in the signature coefficient, the attenuation index, and the retained likelihood-ratio fraction.



Cohort	Records	Eligible	Joint set	C1 set	C1 events
LUAD	522	513	495	477	169
LUSC	504	498	487	477	207
HNSC	528	527	506	432	182
KIRC	537	537	498	495	167
BLCA	412	408	393	391	170
LIHC	377	375	356	332	111
BRCA	1,097	1,091	1,043	1,020	133
STAD	443	437	394	367	142
SKCM	470	455	443	399	186
OV	587	538	375	375	233
LGG	515	514	507	507	125
GBM	596	595	145	145	114
Total	6,588	6,488	5,642	5,417	1,939

Figure 2: Patient selection. The flow diagram shows the cohort-level transition from 6,588 TCGA-CDR records to 5,417 complete cases in the primary analysis, including 1,939 deaths.

group-B reference sets. Two additional group-A signatures were excluded because their gene coverage did not meet the scoring rule [52, 98]. One included necroptosis-related lncRNA signature could not be scored in OV because one component gene had zero variance in that cohort. Thus, 53 published signatures and six reference sets were scored, yielding 59 distinct scored sets.

The group-A category counts are: immune (8), stromal/EMT/CAF (7), proliferation/cell cycle (6), hypoxia (7), ferroptosis/cell death (4), DNA repair/genomic instability (7), metabolism (9), lncRNA/non-coding (3), and other (3). The corresponding cited source papers are immune [14, 17, 45, 63, 78, 79, 95, 102]; stromal/EMT/CAF [10, 12, 57, 66, 74, 94, 97]; proliferation/cell cycle [46, 49, 51, 87, 99, 107]; hypoxia [15, 29, 44, 50, 62, 84, 93]; ferroptosis/cell death [13, 83, 104, 111]; DNA repair/genomic instability [11, 30, 48, 59, 60, 65, 103]; metabolism [40, 54, 55, 58, 61, 106, 112, 114, 115]; lncRNA/non-coding [96, 108, 109]; and other [16, 90, 110].

Group B comprises the ESTIMATE immune and stromal lists [101], the tumour inflammation signature with 18 genes (TIS18) [21, 22], the ten-gene cytotoxic set [21], the 31-gene cell-cycle progression score (ccp31) [20], and the top 15 genes of the Buffa hypoxia metagene [7]. The two coverage-excluded sources are [52, 98]. Table 2 reconciles category counts and pair counts. A full citation-level inventory and provenance status are provided in the supplementary audit file.

Table 1: Characteristics of the primary analysis set in each of the 12 cohorts. Follow-up is the reverse Kaplan–Meier estimate. Age and ABSOLUTE purity are median (Q1, Q3). Stage percentages refer to patients with recorded AJCC stage; stage was unavailable for OV, LGG, and GBM. Pairs A/B are published signatures/reference sets.

Cohort	Patients	Deaths	Follow-up (y)	Age (y)	Female (%)	Stage I–II / III / IV (%)	ABSOLUTE purity	Pairs A/B
LUAD	477	169	2.3	66 (59, 73)	54	79 / 16 / 5	0.45 (0.32, 0.58)	7/6
LUSC	477	207	3.0	68 (62, 73)	26	81 / 17 / 1	0.50 (0.36, 0.65)	2/6
HNSC	432	182	2.8	61 (53, 68)	27	22 / 19 / 60	0.49 (0.37, 0.63)	3/6
KIRC	495	167	4.5	61 (52, 70)	36	60 / 24 / 15	0.56 (0.44, 0.65)	4/6
BLCA	391	170	2.4	69 (60, 76)	26	33 / 35 / 32	0.61 (0.42, 0.80)	5/6
LIHC	332	111	2.1	61 (51, 68)	31	75 / 23 / 1	0.73 (0.55, 0.84)	8/6
BRCA	1,020	133	2.5	58 (49, 67)	99	75 / 24 / 2	0.59 (0.45, 0.74)	5/6
STAD	367	142	1.9	67 (58, 72)	36	46 / 44 / 10	0.52 (0.34, 0.65)	4/6
SKCM	399	186	5.9	60 (48, 71)	38	54 / 41 / 5	0.71 (0.50, 0.85)	2/6
OV	375	233	6.5	58 (51, 68)	100	NA	0.81 (0.70, 0.89)	3/6
LGG	507	125	2.3	41 (32, 53)	44	NA	0.75 (0.61, 0.84)	6/6
GBM	145	114	2.6	62 (53, 70)	35	NA	0.80 (0.65, 0.88)	8/6

Weighted signatures were scored using the published linear predictor, requiring every gene in the model to be present. Unweighted sets were scored as the mean of within-cohort gene z-scores and required at least 80% gene coverage. Scores were standardised to unit standard deviation within each cohort, so hazard ratios represent a one-standard-deviation score difference and are not directly comparable as effect sizes across cohorts. The alternative scoring setting used single-sample gene-set enrichment for unweighted sets and a weighted sum of within-cohort z-scored genes for weighted signatures [4, 47]. Gene symbols and coefficients were checked against the corresponding source publications.

3.4 Purity estimators and Cox models

For each signature–cohort pair, we fitted four nested Cox proportional-hazards models with Efron handling of ties [19, 27]. Let Z denote the retained clinical covariates, P the purity estimate, and S the standardised signature score. The full model is

$$h(t \mid Z, P, S) = h_0(t) \exp\{\gamma^T Z + \theta P + \beta S\}. \tag{1}$$

Model M0 contains clinical covariates only; M1 adds the signature score; M2 adds purity; and M3 contains both purity and the signature score. All models for a given pair were fitted to the same analysis set. The covariates are age at diagnosis per ten years, sex, and AJCC stage I–IV where available. Sex is omitted for BRCA and OV because one sex contributed fewer than ten events. Stage is unavailable for OV, LGG, and GBM.

3.5 Estimands and classification

The primary estimand is the change in the signature coefficient after adding purity:

$$\Delta = \beta_2 - \beta_1, \tag{2}$$

where β_1 is the signature coefficient in M1 and β_2 is the coefficient in M3. Positive Δ means the coefficient is larger after adjustment. Because the same change has different interpretations for protective and harmful signatures, we define an attenuation index

$$A = -\operatorname{sign}(\beta_1)\Delta, \tag{3}$$

so $A > 0$ indicates movement towards zero and $A < 0$ movement away from zero. A third estimand is the retained likelihood-ratio fraction

$$F = \frac{LR(S \mid M2)}{LR(S \mid M0)}, \tag{4}$$

where $LR(S \mid M)$ is the likelihood-ratio statistic for adding the signature to model M. We interpret F only when the unadjusted likelihood-ratio statistic exceeds 3.841, the 5% chi-squared critical value with one degree of freedom; this condition holds for 74 of 129 pairs.

A pair is classified as attenuated when the bootstrap interval of A is entirely positive, amplified when it is entirely negative, and not distinguishable otherwise. A signature association is called largely retained when the BH-adjusted P value for β_2 is below 0.05 and $F \geq 0.5$. Benjamini–Hochberg correction is applied in three families per setting: score–purity association, unadjusted signature coefficient, and adjusted signature coefficient [5]. These categories are descriptive; they do not identify causal confounding.

3.6 Expression-matched random-signature null

For every signature–cohort pair, we generated 1,000 random gene sets matched to the signature size and mean expression within ten expression-level strata. Each random set is scored and analysed using the same models, producing reference distributions for Δ and the hazard ratio. The observed coefficient change is compared with these distributions. The random-set comparison serves as a calibration device rather than a causal test.

3.7 Sensitivity settings

The primary setting C1 uses ABSOLUTE purity and the primary scoring method. Four sensitivity settings are described: C2 replaces ABSOLUTE with consensus purity estimates (CPE); C3 uses ESTIMATE purity; C4 uses the alternative scoring method; and C5 adjusts for age and sex only, omitting stage to retain patients with missing stage. Sensitivity settings C2–C5 used 200 bootstrap replicates. C2 includes 119 pairs because STAD has no CPE value; C3 and C4 include 129 pairs; C5 includes 94 pairs because it differs

Table 2: Gene sets by biological category. Group A counts included published signatures; group B counts reference sets. The last row gives the two additional published signatures excluded for insufficient coverage.

Category	Group A	Group B	Signature–cohort pairs
Immune	8	3	44
Stromal, EMT and CAF	7	1	19
Proliferation and cell cycle	6	1	19
Hypoxia	7	1	21
Ferroptosis and cell death	4	0	4
DNA repair and genomic instability	7	0	8
Metabolism	9	0	9
lncRNA and non-coding	3	0	2
Other	3	0	3
Not scored (gene coverage)	2	0	0
Included totals (excluding coverage-excluded row)	54	6	129

from C1 only in cohorts with a stage variable. In C3, 38 pairs are flagged as circular because the immune or stromal signature genes overlap with genes used by ESTIMATE.

3.8 Diagnostics and synthesis

We assessed proportional-hazards assumptions using scaled Schoenfeld residuals [36], evaluated non-linearity with spline checks, tested signature-by-purity interactions, inspected martingale residuals, summarised results by purity tertile, and calculated five-year restricted mean survival time (RMST) contrasts for flagged pairs. Sensitivity analyses are also described for zero overall-survival times and for ABSOLUTE calls without quality flags. Ten signatures scored in at least two cohorts (six reference sets across twelve cohorts and four glioma signatures across LGG and GBM) were pooled using a DerSimonian–Laird random-effects meta-analysis with Hartung–Knapp intervals. Category effects were summarised using a restricted maximum-likelihood mixed model with a random intercept for signature.

3.9 Signature provenance and TCGA overlap

The inventory contained 62 entries: 54 included published signatures, six reference sets, and two published signatures excluded for insufficient gene coverage. At the signature level, 52 entries overlapped TCGA training samples, eight did not, one partly overlapped, and one had unknown overlap status. At the pair level, 73 of 129 C1 pairs were classified as overlapping and 43 as non-overlapping, leaving 13 pairs without an explicit pair-level overlap classification. These 13 pairs were retained as unassigned rather than allocated to an overlap category.

A targeted bibliographic review examined recent 2025–2026 references. Publication records and DOI metadata were checked for the recent references listed in the supplementary audit. Several publications used the same TCGA cohort as the present analysis, including the 2026 ovarian p-EMT signature in TCGA-OV, the gastric ferroptosis/ER-stress signature in TCGA-STAD, the bladder amino-acid-metabolism signature in TCGA-BLCA, and the LUAD galactose-metabolism signature in TCGA-LUAD. One 2026 four-gene glioma cell-cycle study used CGGA mRNAseq cohorts rather than TCGA and was not classified as direct TCGA overlap based on its reported data sources.

4 Results

4.1 Cohorts and signature inventory

The primary analysis included 5,417 complete cases and 1,939 deaths across the twelve cohorts (Table 1, Figure 2). Cohort sizes range from 145 patients in GBM to 1,020 in BRCA. The number of published-signature pairs per cohort ranges from two in LUSC and SKCM to eight in LIHC and GBM; each cohort also contributes six reference-set pairs.

The signature inventory contains 54 included published signatures and six reference sets, with two additional published signatures excluded for insufficient gene coverage. One included ovarian necroptosis-related lncRNA signature was not scored in OV because one component gene had zero variance. Overall, 53 published signatures and six reference sets were scored (59 distinct scored sets). The pair counts in Table 2 sum to 129. Table 1 reports 57 group-A pairs and 72 group-B pairs across cohorts, also summing to 129.

4.2 Association between signature scores and purity

Signature scores were associated with ABSOLUTE purity after BH correction in 97 of 129 pairs. The median absolute Pearson correlation was 0.28; 63 pairs had $|r| \geq 0.30$, and correlations ranged from −0.69 to 0.57. Immune and stromal signatures showed the strongest negative correlations with purity (median $r = -0.47$ and $r = -0.46$, respectively). Proliferation signatures showed a weak positive median correlation ($r = 0.16$), while the median correlations for hypoxia, ferroptosis, DNA repair, and metabolism categories were within 0.08 of zero.

4.3 Change in the prognostic coefficient after purity adjustment

The median unadjusted hazard ratio was 1.24 per standard deviation of the signature score. The BH-adjusted P value for the signature coefficient was below 0.05 in 71 of 129 pairs in M1 and in 71 pairs in

M3; 68 pairs were significant in both. Three pairs were significant only in M1 and three only in M3. Seventy-one pairs met the source definition of a largely retained association, although two had no interpretable retained fraction because the unadjusted likelihood-ratio statistic did not exceed the stated threshold.

The coefficient change was small for most pairs. The median Δ was 0.003, median $|\Delta|$ was 0.022, the largest $|\Delta|$ was 0.172, and the median attenuation index was −0.006. Based on the bootstrap intervals, four pairs were attenuated, 13 were amplified, and 112 were not distinguishable from zero (Figure 3, Table 3). All four attenuated pairs were group-B reference sets: the SKCM ESTIMATE stromal set, LUAD TIS18, SKCM Buffa hypoxia15, and SKCM ccp31. No group-A published prognostic signature was classified as attenuated.

The 13 amplified pairs comprised seven group-A signatures and six group-B sets. The group-A examples are the LUAD DNA-damage-response checkpoint signature, LUAD extracellular-matrix signature, OV partial-EMT signature, OV oxidative-phosphorylation signature, LIHC inflammatory signature, LIHC hypoxia signature, and GBM mitotic four-gene signature. Eleven of the 13 amplified pairs had negative score–purity correlations. Several had unadjusted coefficients close to zero that increased after adjustment; the reported KIRC TIS18 hazard ratio, for example, changed from 0.90 to 0.79.

4.4 Comparison with expression-matched random gene sets

Observed attenuation exceeded the upper tail of the expression-matched random-set distribution at nominal $P < 0.05$ in 15 pairs and in 10 pairs after BH correction. All ten corrected pairs were group-B immune or stromal reference sets: ESTIMATE stromal in LUAD, HNSC, and SKCM; ESTIMATE immune in LUAD, BLCA, and STAD; TIS18 in LUAD and LIHC; and cytotoxic10 in LUAD and OV. No group-A published signature exceeded the random reference after correction. Among 25 pairs using purity-linked control sets, nine exceeded the reference at nominal $P < 0.05$, compared with six of the other 104 pairs. The observed Δ lay outside the central 95% interval of the random-set changes in 50 of 129 pairs (27 above and 23 below), including amplification as well as attenuation.

4.5 Dependence on purity estimator and scoring method

The unadjusted coefficient β_1 was stable across settings, with Spearman correlations against C1 of 0.996 for CPE, 0.995 for ESTIMATE, 0.963 for alternative scoring, and 0.985 for age-and-sex-only adjustment. The coefficient change Δ was less stable: correlations with C1 were 0.73, 0.56, 0.84, and 0.93, respectively. Class agreement was 0.87, 0.76, 0.93, and 0.93, with Cohen's κ values of 0.54, 0.14, 0.71, and 0.72. The class differed among the three purity estimators in 37 of 129 pairs. Table 4 and Figure 4 summarise the sensitivity analyses.

Median within-cohort Spearman correlations were 0.76 between ABSOLUTE and CPE (range 0.41–0.83 across 11 cohorts), 0.67 between ABSOLUTE and ESTIMATE (0.36–0.79 across 12 cohorts), and 0.82 between CPE and ESTIMATE (0.69–0.92 across 11 cohorts). In C3, 38 pairs use immune (32) or stromal (six) signatures that share genes with ESTIMATE purity. Among these 38 pairs, three were attenuated, four amplified, and 31 not distinguishable; among the other 91 pairs, the corresponding counts were nine, eight, and 74. The number of attenuated pairs was 10 in C2, 12 in C3, three in C4, and eight in C5, compared with four in C1.

4.6 Category-level results and heterogeneity

Table 5 summarises the category-level results. Immune and stromal signatures showed the strongest correlations with purity and accounted for most pairs whose attenuation exceeded the random reference. Thirteen of 44 immune pairs and 10 of 19 stromal pairs had significant unadjusted hazard ratios. All seven DNA-repair pairs and all nine metabolism pairs that were significant in M1 remained significant in M3. The ferroptosis (four pairs), lncRNA (two pairs), and other (three pairs) categories were considered too small for category-level conclusions.

For the six reference sets scored across all twelve cohorts, the sign of the unadjusted coefficient was shared by nine of twelve cohorts for TIS18, ccp31, cytotoxic10, and Buffa hypoxia15; eight cohorts for ESTIMATE stromal; and seven for ESTIMATE immune. The attenuation-index range across cohorts was 0.11 for Buffa hypoxia15 and 0.27 for ESTIMATE immune. SKCM contributed three of the four attenuated pairs, while KIRC and OV contributed most amplified pairs. OV had the highest median purity (0.81) and the narrowest interquartile range (0.19).

The random-effects meta-analysis of Δ for the ten sets scored in at least two cohorts yielded no pooled interval excluding zero under either Wald or Hartung–Knapp intervals. The median I^2 was 25%, and no Cochran Q test was below 0.05. In the category mixed model, the omnibus test of category differences had likelihood-ratio statistic 1.76 on eight degrees of freedom ($P = 0.99$). Eight of nine category means were below zero; only the proliferation category had an interval excluding zero (mean $A = -0.021$, 95% CI −0.041 to −0.002), without correction for nine categories. The estimated signature variance was at the boundary of the parameter space.

4.7 Diagnostics, quality filters, and training-data overlap

The Grambsch–Therneau proportional-hazards test flagged 12 of 129 pairs, close to the 13 expected by chance among 258 tests. For these pairs, the five-year RMST difference between patients above and below the cohort median was negative with an interval excluding zero in eight pairs and including zero in four. The largest reported differences were for the LGG DNA-damage-response signature (−438 days, 95% CI −548 to −328) and the LIHC inflammatory signature (−268 days, 95% CI −437 to −99). The signature-by-purity interaction test was below 0.05 in seven of 129 pairs, and the spline test for non-linearity in purity was below 0.05 in nine pairs.

Excluding patients with overall-survival time equal to zero left the sign of β_1 unchanged in all 129 pairs; the largest change in Δ was 0.002 and the largest absolute change was 0.088, with all such changes inside the primary bootstrap intervals. Restricting ABSOLUTE calls to those without quality flags removed zero to 169 patients and changed 110 pairs. The sign of β_1 changed in three pairs (LUSC cytotoxic10, LUSC Buffa hypoxia, and OV ccp31), each with an unadjusted coefficient close to zero; the median change in Δ was 0.004.

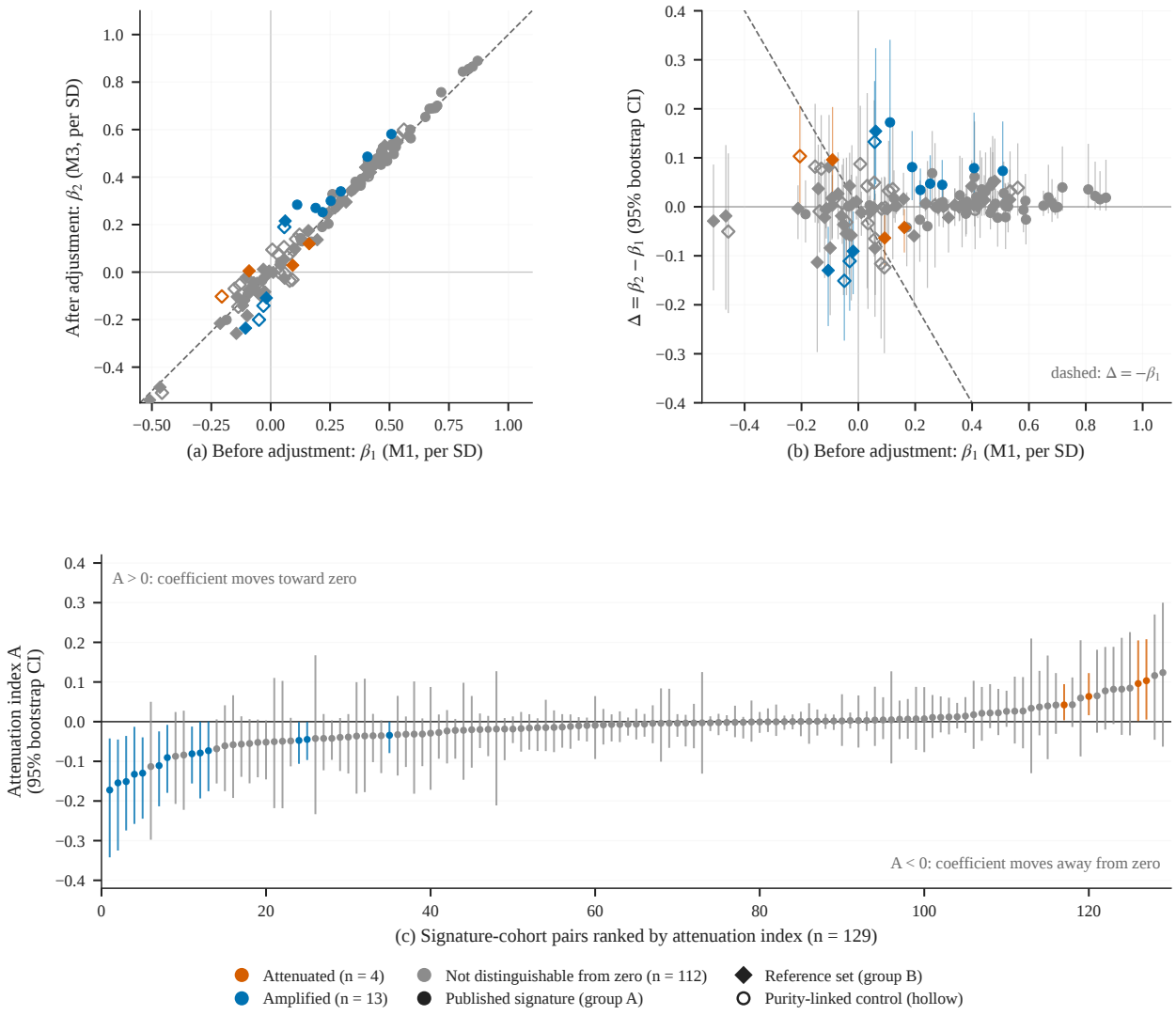


Figure 3: Primary-setting coefficient comparisons. Panel (a) plots the adjusted log hazard ratio against the unadjusted log hazard ratio; panel (b) plots the coefficient change and its 95% bootstrap interval; panel (c) ranks the 129 pairs by attenuation index.

Table 3: The four pairs classified as attenuated in C1. HR1 and HR2 are hazard ratios per standard deviation before and after purity adjustment. Coefficient changes have 95% bootstrap intervals. C2–C4 classes are the sensitivity classifications.

Pair	Patients	r	HR1 (95% CI)	HR2 (95% CI)	Δ (95% bootstrap CI)	A	C2	C3	C4
SKCM, ESTIMATE stromal	399	−0.46	0.81 (0.70, 0.94)	0.90 (0.76, 1.07)	0.103 (0.008, 0.205)	0.103	Att.	Att.	Att.
LUAD, TIS18 immune	477	−0.53	0.91 (0.78, 1.06)	1.01 (0.85, 1.19)	0.096 (0.004, 0.203)	0.096	N.d.	N.d.	N.d.
SKCM, Buffa hypoxia15	399	0.23	1.10 (0.93, 1.30)	1.03 (0.87, 1.22)	−0.064 (−0.120, −0.019)	0.064	Att.	Att.	Att.
SKCM, ccp31 (31 genes)	399	0.20	1.18 (1.00, 1.38)	1.13 (0.96, 1.32)	−0.042 (−0.092, −0.006)	0.042	Att.	Att.	Att.

Of the 62 inventory entries, 52 overlapped with TCGA samples, eight were non-overlapping, one partly overlapped, and one had unknown overlap status. In C1, 73 pairs were labelled as overlapping and 43 as non-overlapping. These pair counts sum to 116, leaving 13 of the 129 pairs without an explicit pair-level overlap category. Overlap is also associated with signature group because the reference sets were defined independently of TCGA outcomes and the non-overlapping sets are mainly group-B controls. The unclassified pairs are therefore retained as unassigned in the overlap summary.

Table 4: Classification of coefficient change in the primary and four sensitivity settings. C2–C5 use 200 bootstrap replicates.

Setting	Pairs	Bootstrap B	Attenuated	Amplified	Not dist.	Median $\lvert r \rvert$	Spearman	Agreement	Kappa
C1, ABSOLUTE purity, primary score	129	1,000	4	13	112	0.28	–	–	–
C2, CPE purity	119	200	10	13	96	0.36	0.73	0.87	0.54
C3, ESTIMATE purity	129	200	12	12	105	0.43	0.56	0.76	0.14
C4, Alternative scoring	129	200	3	15	111	0.30	0.84	0.93	0.71
C5, Age and sex only	94	200	8	8	78	0.31	0.93	0.93	0.72

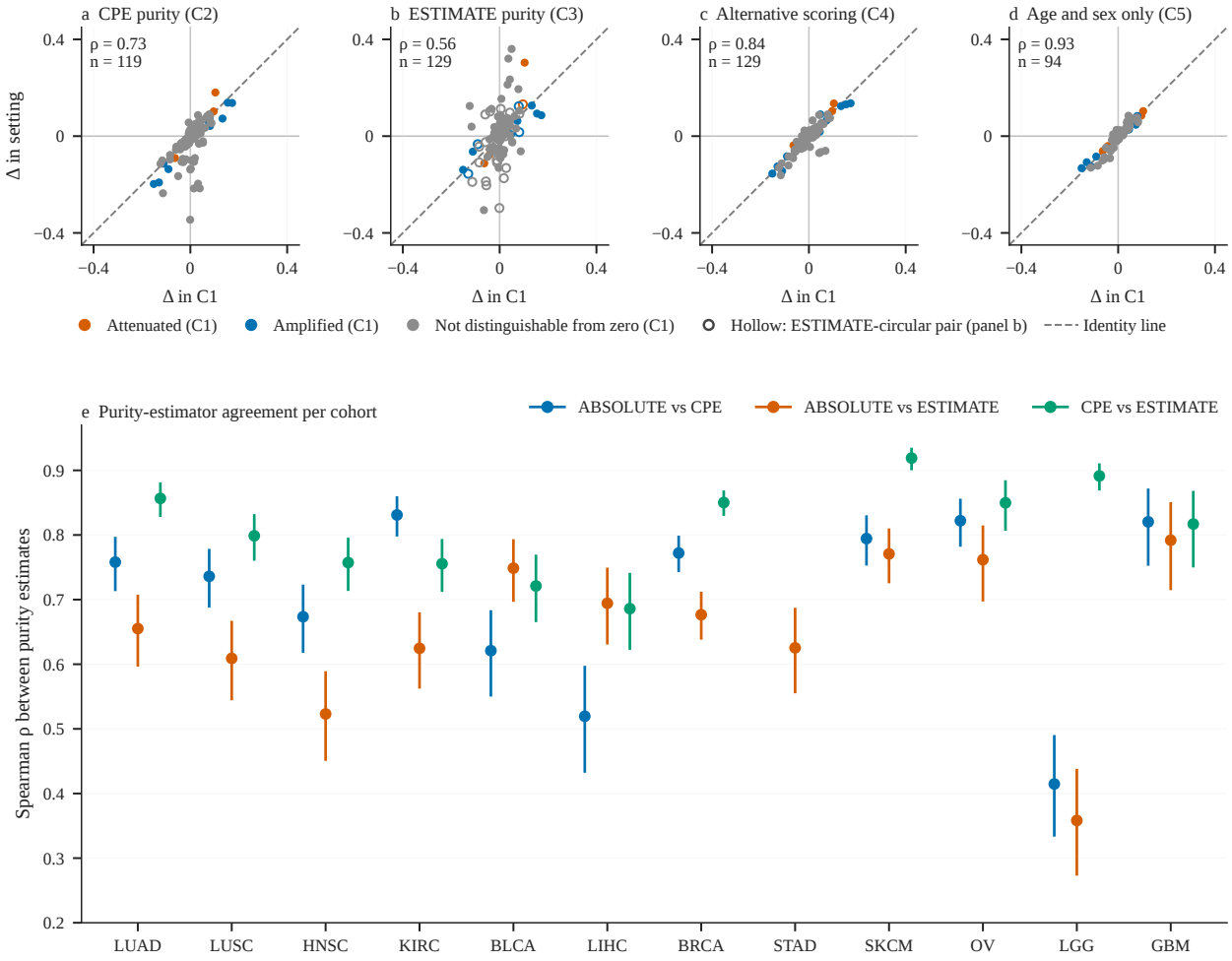


Figure 4: Sensitivity of coefficient change to purity estimator and scoring. Panels (a)–(d) compare C2–C5 with C1; panel (e) shows within-cohort Spearman correlations between purity estimators.

5 Discussion

The results indicate that adding ABSOLUTE purity changed most prognostic signature coefficients by an amount that the bootstrap intervals could not distinguish from zero. The four pairs classified as attenuated were reference sets describing immune, stromal, proliferative, or hypoxic programmes; none of the 53 scored published signatures was among them. More pairs were amplified than attenuated. This pattern is consistent with the possibility that many published signatures retain prognostic associations beyond a single scalar purity measure, but it does not establish that those associations are tumour-cell intrinsic. Purity summarises the total non-malignant fraction and does not resolve its cellular composition. A signature can therefore capture biologically meaningful microenvironmental signal that is not removed by a single purity covariate [25, 56, 71, 76].

Table 5: Results by biological category in the primary setting. Median r is the median Pearson correlation between score and ABSOLUTE purity. Significance columns count BH-adjusted $P < 0.05$ for the signature hazard ratio in M1 and M3. The last column is the REML category mean of the attenuation index.

Category	Pairs	Sets	Median r	M1 sig.	M3 sig.	Atten./amplif.	Beyond null	Mean attenuation index (95% CI)
Immune	44	11	−0.47	13	14	1/4	7	−0.013 (−0.028, 0.002)
Stromal, EMT and CAF	19	8	−0.46	10	8	1/4	3	−0.012 (−0.034, 0.010)
Proliferation and cell cycle	19	7	0.16	10	10	1/2	0	−0.021 (−0.041, −0.002)
Hypoxia	21	8	−0.08	13	13	1/1	0	−0.004 (−0.024, 0.016)
Ferroptosis and cell death	4	4	0.07	4	4	0/0	0	−0.010 (−0.061, 0.040)
DNA repair and genomic instability	8	7	−0.04	7	8	0/1	0	−0.022 (−0.057, 0.014)
Metabolism	9	9	−0.07	9	9	0/1	0	−0.009 (−0.042, 0.025)
lncRNA and non-coding	2	2	−0.07	2	2	0/0	0	−0.009 (−0.080, 0.062)
Other	3	3	0.29	3	3	0/0	0	0.000 (−0.058, 0.058)

The direction of coefficient change also requires care. The attenuation index changes sign according to the original coefficient, so positive values indicate movement towards zero for both protective and harmful signatures. A coefficient can move away from zero after adjustment when the signature score and purity are correlated and their outcome associations differ. Hazard ratios may also change after adding covariates for reasons other than confounding, including the conditional nature of the Cox model and non-collapsibility [37, 41, 77, 91]. The terms attenuation and amplification in this manuscript therefore describe statistical movement, not biological mechanisms.

The random-set comparison provides an additional calibration. The pairs exceeding the random-set reference after correction were all immune or stromal reference sets, which are precisely the sets most closely connected to the construction of expression-derived purity measures. This supports caution when interpreting immune and stromal controls, especially under ESTIMATE, where signature genes and purity genes can overlap by design. The absence of a published group-A signature among the corrected attenuated pairs does not imply that published signatures are free of microenvironmental influence.

The sensitivity results indicate that the coefficient change is less stable than the unadjusted coefficient. The Spearman correlation between C1 and ESTIMATE coefficient changes was 0.56, and class agreement of 0.76 with kappa 0.14. Agreement among the purity estimators is moderate. A conclusion based on one estimator may therefore be fragile. The choice of purity measure should be reported alongside the score, cohort, and model specification rather than treated as a technical detail.

The category analysis does not support a general ranking of biological signature classes by susceptibility to purity adjustment. The omnibus category test was not significant, and the category sizes for ferroptosis, lncRNA, and other signatures were small. The category-level mixed model also estimated signature variance at the boundary, limiting the separation of between-signature and residual variation. Similarly, the lack of detected heterogeneity in the random-effects meta-analysis does not prove that the cohorts agree, particularly when only ten sets contribute repeated-cohort information.

5.1 Study limitations

Several limitations should be considered. First, the analysis is retrospective and based on TCGA cohorts. Fifty-two of the 62 inventory entries overlapped with TCGA samples used for signature derivation or evaluation; these results therefore do not constitute independent external validation. Second, purity is a scalar estimate and cannot represent all components of the tumour microenvironment. Third, expression scales and gene annotations may differ from those used in the original signature papers. The alternative within-cohort scoring procedure was intended to reduce, but not eliminate, this mismatch.

Fourth, the primary setting (C1) used 1,000 bootstrap replicates, whereas sensitivity settings C2–C5 used 200. The smaller number of replicates in the sensitivity analyses may yield less stable interval estimates and should be considered when comparing settings. Fifth, 73 overlapping and 43 non-overlapping pairs were classified at the pair level, leaving 13 of 129 pairs without an explicit overlap category. These pairs remain unassigned in the overlap summary. Finally, the targeted bibliographic review verified publication and DOI metadata for recent references and identified several instances of TCGA cohort reuse; the pair-level overlap classifications should therefore be interpreted alongside the unassigned cases described above.

5.2 Implications for reporting

Future signature studies should report the unadjusted and purity-adjusted hazard ratios together with uncertainty intervals, the exact purity estimator, the scoring rule, the number of patients and events, the gene coverage, and the overlap between the signature's derivation data and the validation cohort. A random-set reference can help distinguish a signature-specific coefficient change from the changes expected for expression-matched gene sets, but it should be treated as a calibration device rather than a causal test. Where possible, analyses should use an independent validation cohort and a purity estimator that does not reuse the expression features of the signature. These reporting recommendations are consistent with the broader emphasis on transparent prognostic-marker evaluation and reproducibility [18, 26, 68, 69, 73, 85, 89].

6 Conclusion

This pan-cancer audit evaluated 129 signature–cohort pairs across twelve TCGA cohorts. Purity adjustment generally produced small coefficient changes: four pairs were attenuated, all belonging to

reference sets, while thirteen pairs were amplified. The magnitude and classification of coefficient changes depended on the purity estimator. These findings support reporting purity-adjusted and unadjusted associations side by side, together with uncertainty intervals and expression-matched random-set comparisons. They do not establish a causal role for purity or for any individual signature. Overall, the results highlight the importance of considering tumour purity when interpreting prognostic transcriptomic signatures while recognising that a single purity covariate cannot capture the full complexity of the tumour microenvironment.

References

[1] Dvir Aran, Zicheng Hu, and Atul J. Butte. 2017. xCell: digitally portraying the tissue cellular heterogeneity landscape. Genome Biology 18, 1 (2017), 220.

[2] Dvir Aran, Marina Sirota, and Atul J. Butte. 2015. Systematic pan-cancer analysis of tumour purity. Nature Communications 6, 1 (2015), 8971.

[3] Francisco Avila Cobos, José Alquicira-Hernandez, Joseph E. Powell, Pieter Mestdagh, and Katleen De Preter. 2020. Benchmarking of cell type deconvolution pipelines for transcriptomics data. Nature Communications 11, 1 (2020), 5650.

[4] David A. Barbie, Pablo Tamayo, Jesse S. Boehm, So Young Kim, Susan E. Moody, Ian F. Dunn, et al. 2009. Systematic RNA interference reveals that oncogenic KRAS-driven cancers require TBK1. Nature 462, 7269 (2009), 108– 112.

[5] Yoav Benjamini and Yosef Hochberg. 1995. Controlling the False Discovery Rate: A Practical and Powerful Approach to Multiple Testing. Journal of the Royal Statistical Society Series B: Statistical Methodology 57, 1 (1995), 289– 300.

[6] Bhavneet Bhinder, Verena Friedl, Sunantha Sethuraman, Davide Risso, Kami E. Chiotti, R. Jay Mashl, et al. 2025. Pan-cancer immune and stromal deconvolution predicts clinical outcomes and mutation profiles. Scientific Reports 15, 1 (2025), 23921. DOI: https://doi.org/10.1038/s41598-025-09075-y.

[7] F M Buffa, A L Harris, C M West, and C J Miller. 2010. Large meta-analysis of multiple cancers reveals a common, compact and highly prognostic hypoxia metagene. British Journal of Cancer 102, 2 (2010), 428–435.

[8] Alexandre Calon, Enza Lonardo, Antonio Berenguer-Llergo, Elisa Espinet, Xavier Hernando-Momblona, Mar Iglesias, et al. 2015. Stromal gene expression defines poor-prognosis subtypes in colorectal cancer. Nature Genetics 47, 4 (2015), 320–329.

[9] Scott L Carter, Kristian Cibulskis, Elena Helman, Aaron McKenna, Hui Shen, Travis Zack, et al. 2012. Absolute quantification of somatic DNA alterations in human cancer. Nature Biotechnology 30, 5 (2012), 413–421.

[10] Yanfei Chai, Yuchao Ma, Wei Feng, Hong Xiang, Hongwei Lu, and Longyu Jin. 2024. Identification and validation of a 4-extracellular matrix gene signature associated with prognosis and immune infiltration in lung adenocarcinoma. Heliyon 10, 2 (2024), e24162.

[11] Yiming Chang, Zhiyuan Huang, Hong Quan, Hui Li, Shuo Yang, Yifei Song, Jian Wang, Jian Yuan, and Chenming Wu. 2023. Construction of a DNA damage repair gene signature for predicting prognosis and immune response in breast cancer. Frontiers in Oncology 12 (2023), 1085632.

[12] Chia-Chia Chao, Cheng-Yao Lin, Po-Chun Chen, Wen-Tsung Huang, Teng-Song Weng, and Sheng-Yen Hsiao. 2026. A Novel Partial EMT-Associated Transcriptomic Signature for Prognostic Stratification in Ovarian Cancer. Oncology Research 34, 5 (2026), 27. DOI: https://doi.org/10.32604/or.2026.074383.

[13] Hongyu Chen, Zhilei Chen, Ke Cao, and Zhenjun Wang. 2026. A novel ferroptosisand endoplasmic reticulum stress-related gene signature for predicting prognosis, immune features and drug sensitivity in gastric cancer. Discover Oncology 17, 1 (2026), 403. DOI: https://doi.org/10.1007/s12672-026-04562-8.

[14] Haitao Chen, Yueying Li, Shu-Yuan Xiao, and Jianchun Guo. 2021. Identification of a five-immune gene model as an independent prognostic factor in hepatocellular carcinoma. BMC Cancer 21, 1 (2021), 278.

[15] Hualin Chen, Yang Pan, Xiaoxiang Jin, and Gang Chen. 2021. Identification of a Four Hypoxia-Associated Long Non-Coding RNA Signature and Establishment of a Nomogram Predicting Prognosis of Clear Cell Renal Cell Carcinoma. Frontiers in Oncology 11 (2021), 713346.

[16] Mei Chen, Shufang Zhang, Zhenyu Nie, Xiaohong Wen, and Yuanhui Gao. 2020. Identification of an Autophagy-Related Prognostic Signature for Clear Cell Renal Cell Carcinoma. Frontiers in Oncology 10 (2020), 873.

[17] Yan Chen, Yiqing You, Qiaoling Wu, Jing Wu, Shujing Lin, Yang Sun, and Zhaolei Cui. 2023. Performance of a PLK1-based immune risk model for prognosis and treatment response prediction in breast cancer. Cancer Medicine 12, 9 (2023), 11020–11039.

[18] Gary S Collins, Karel G M Moons, Paula Dhiman, Richard D Riley, Andrew L Beam, Ben Van Calster, et al. 2024. TRIPOD+AI statement: updated guidance for reporting clinical prediction models that use regression or machine learning methods. BMJ 385 (2024), e078378.

[19] D. R. Cox. 1972. Regression Models and Life-Tables. Journal of the Royal Statistical Society Series B: Statistical Methodology 34, 2 (1972), 187–202.

[20] Jack Cuzick, Gregory P Swanson, Gabrielle Fisher, Arthur R Brothman, Daniel M Berney, Julia E Reid, et al. 2011. Prognostic value of an RNA expression signature derived from cell cycle proliferation genes in patients with prostate cancer: a retrospective study. The Lancet Oncology 12, 3 (2011), 245– 255.

[21] Patrick Danaher, Sarah Warren, Lucas Dennis, Leonard D'Amico, Andrew White, Mary L. Disis, Melissa A. Geller, Kunle Odunsi, Joseph Beechem, and Steven P. Fling. 2017. Gene expression markers of Tumor Infiltrating Leukocytes. Journal for ImmunoTherapy of Cancer 5, 1 (2017), 18.

[22] Patrick Danaher, Sarah Warren, Rongze Lu, Josue Samayoa, Amy Sullivan, Irena Pekker, Brett Wallden, Francesco M. Marincola, and Alessandra Cesano. 2018. Pan-cancer adaptive immune resistance as defined by the Tumor Inflammation Signature (TIS): results from The Cancer Genome Atlas (TCGA). Journal for ImmunoTherapy of Cancer 6, 1 (2018), 63.

[23] Leepakshi Dhingra, Manulaya Singh, Simran Jit, Deepika Yadav, and Sherry Bhalla. 2026. Systematic Meta-Analysis of Published Transcriptomic Prognostic Signatures and Development of a Robust Multi-Cohort Prognostic Classifier for Triple-Negative Breast Cancer. bioRxiv preprint (2026). DOI: https://doi.org/10.64898/2026.07.09.737472.

[24] Matteo Di Giovannantonio, Fiona Hartley, Badran Elshenawy, Alessandro Barberis, Dan Hudson, Hana S. Shafique, et al. 2025. Defining hypoxia in cancer: A landmark evaluation of hypoxia gene expression signatures. Cell Genomics 5, 2 (2025), 100764. DOI: https://doi.org/10.1016/j.xgen.2025.100764.

[25] Philip D. Dunne, Matthew Alderdice, Paul G. O'Reilly, Aideen C. Roddy, Amy M. B. McCorry, Susan Richman, et al. 2017. Cancer-cell intrinsic gene expression signatures overcome intratumoural heterogeneity bias in colorectal cancer patient classification. Nature Communications 8, 1 (2017), 15657.

[26] Alain Dupuy and Richard M. Simon. 2007. Critical Review of Published Microarray Studies for Cancer Outcome and Guidelines on Statistical Analysis and Reporting. JNCI: Journal of the National Cancer Institute 99, 2 (2007), 147–157.

[27] Bradley Efron. 1977. The Efficiency of Cox's Likelihood Function for Censored Data. J. Amer. Statist. Assoc. 72, 359 (1977), 557–565.

[28] Liat Ein-Dor, Itai Kela, Gad Getz, David Givol, and Eytan Domany. 2005. Outcome signature genes in breast cancer: is there a unique set? Bioinformatics 21, 2 (2005), 171–178.

[29] Xiang Fang, Xinhao Wu, and Chengran Xu. 2025. Characterization of hypoxia-related molecular clusters and prognostic riskScore for glioma. Frontiers in Oncology 15 (2025), 1605949. DOI: https://doi.org/10.3389/fonc.2025.1605949.

[30] Jia Feng, Yuankai Si, Long Han, Yilan Huang, and Longyang Jiang. 2026. Identification and validation of biomarkers related to mismatch repair for prognosis prediction in glioma. Frontiers in Immunology 17 (2026), 1652739. DOI: https://doi.org/10.3389/fimmu.2026.1652739.

[31] Greg Finak, Nicholas Bertos, Francois Pepin, Svetlana Sadekova, Margarita Souleimanova, Hong Zhao, et al. 2008. Stromal gene expression predicts clinical outcome in breast cancer. Nature Medicine 14, 5 (2008), 518–527.

[32] Erlend I. F. Fossen, Mauricio Moreira-Soares, Marissa LeBlanc, Arnoldo Frigessi, Eivind Hovig, Laura Lopez-Perez, et al. 2024. External validation of prognostic and predictive gene signatures in head and neck cancer patients. medRxiv preprint (2024).

[33] Jérôme Galon, Anne Costes, Fatima Sanchez-Cabo, Amos Kirilovsky, Bernhard Mlecnik, Christine Lagorce-Pagès, et al. 2006. Type, Density, and Location of Immune Cells Within Human Colorectal Tumors Predict Clinical Outcome. Science 313, 5795 (2006), 1960–1964.

[34] Andrew J Gentles, Aaron M Newman, Chih Long Liu, Scott V Bratman, Weiguo Feng, Dongkyoon Kim, et al. 2015. The prognostic landscape of genes and infiltrating immune cells across human cancers. Nature Medicine 21, 8 (2015), 938–945.

[35] Mary J. Goldman, Brian Craft, Mim Hastie, Kristupas Repečka, Fran McDade, Akhil Kamath, et al. 2020. Visualizing and interpreting cancer genomics data via the Xena platform. Nature Biotechnology 38, 6 (2020), 675–678.

[36] PATRICIA M. GRAMBSCH and TERRY M. THERNEAU. 1994. Proportional hazards tests and diagnostics based on weighted residuals. Biometrika 81, 3 (1994), 515–526.

[37] Sander Greenland, Judea Pearl, and James M. Robins. 1999. Confounding and Collapsibility in Causal Inference. Statist. Sci. 14, 1 (1999), 29–46.

[38] Robert L. Grossman, Allison P. Heath, Vincent Ferretti, Harold E. Varmus, Douglas R. Lowy, Warren A. Kibbe, and Louis M. Staudt. 2016. Toward a Shared Vision for Cancer Genomic Data. New England Journal of Medicine 375, 12 (2016), 1109–1112.

[39] Benjamin Haibe-Kains, Christine Desmedt, Fanny Piette, Marc Buyse, Fatima Cardoso, Laura van't Veer, Martine Piccart, Gianluca Bontempi, and Christos Sotiriou. 2008. Comparison of prognostic gene expression signatures for breast cancer. BMC Genomics 9, 1 (2008), 394.

[40] Junrui He, Xu Liu, Shirui Li, Zhongyou Xia, Xiaojun Tan, Lijuan Peng, Qiongxian Long, and Ji Wu. 2026. A systematic characterization of amino acid metabolism–related genes reveals molecular subtypes and a prognostic signature in bladder

cancer. Frontiers in Oncology 16 (2026), 1754912. DOI: https://doi.org/10.3389/fonc.2026.1754912.

[41] Miguel A. Hernán. 2010. The Hazards of Hazard Ratios. Epidemiology 21, 1 (2010), 13–15.

[42] Kyle J. Hitscherich, Darryl Nousome, Aaron J. Dinerman, Victoria Dulemba, Frank J. Lowery, and Naris Nilubol. 2025. A pan-cancer comparative analysis of the cancer genome atlas transcriptomic TIL-immune signatures. Cancer Immunology, Immunotherapy 74, 9 (2025), 286. DOI: https://doi.org/10.1007/s00262-025-04102-3.

[43] Katherine A. Hoadley, Christina Yau, Toshinori Hinoue, Denise M. Wolf, Alexander J. Lazar, Esther Drill, et al. 2018. Cell-of-Origin Patterns Dominate the Molecular Classification of 10,000 Tumors from 33 Types of Cancer. Cell 173, 2 (2018), 291–304.e6.

[44] Wenhao Hu, Dute Gao, Guojun Hou, Chang Liu, Xianglong Meng, Qinlong Liu, and Jiaan Sun. 2026. A Hypoxia and EMT-Related Gene Signature for Predicting Prognosis and Immunotherapy Benefit in Hepatocellular Carcinoma. Journal of Hepatocellular Carcinoma 13 (2026), Article 642054. DOI: https://doi.org/10.2147/JHC.S642054.

[45] Xiaoliang Hua, Juan Chen, Yang Su, and Chaozhao Liang. 2020. Identification of an immune-related risk signature for predicting prognosis in clear cell renal cell carcinoma. Aging 12, 3 (2020), 2302–2332.

[46] Yongfeng Hui, Junzhi Leng, Dong Jin, Di Liu, Genwang Wang, Qi Wang, and Yanyang Wang. 2021. A Cell Cycle Progression-Derived Gene Signature to Predict Prognosis and Therapeutic Response in Hepatocellular Carcinoma. Disease Markers 2021 (2021), 1–36.

[47] Sonja Hänzelmann, Robert Castelo, and Justin Guinney. 2013. GSVA: gene set variation analysis for microarray and RNA-Seq data. BMC Bioinformatics 14, 1 (2013), 7.

[48] Bin Jia, Ting Gong, Bingsheng Sun, Zhenfa Zhang, Diansheng Zhong, and Changli Wang. 2022. Identification of a DNA damage repair gene-related signature for lung squamous cell carcinoma prognosis. Thoracic Cancer 13, 8 (2022), 1143–1152.

[49] Hongkai Jia, Nan Pu, and Chunyan Tian. 2026. An Interpretable Four-Gene Cell-Cycle Signature Links Malignant Progression to Adverse Survival in Adult Primary Diffuse Glioma: A CGGA Transcriptome Study. Genes 17, 7 (2026), 833. DOI: https://doi.org/10.3390/genes17070833.

[50] Chen Jiang, Xingge Li, Yilin Liu, Sicheng Cai, Hailing Yao, Huiying Shi, Kan Wang, Ying Yao, and Rong Lin. 2026. Integrated Weighted Gene Co-Expression Network and Single-Cell RNA Sequencing Analyses Reveal the Prognostic Significance of Hypoxia in Gastric Cancer. Biomedicines 14, 2 (2026), 425. DOI: https://doi.org/10.3390/biomedicines14020425.

[51] Wei Jiang, Jiameng Xu, Zirui Liao, Guangbin Li, Chengpeng Zhang, and Yu Feng. 2021. Prognostic Signature for Lung Adenocarcinoma Patients Based on Cell-Cycle-Related Genes. Frontiers in Cell and Developmental Biology 9 (2021), 655950.

[52] Ziyu Jiang, Xiaomei Zhuang, Junkui Guo, Minyi Zhu, Chunhong Hong, Chunhui Sun, Kaiming Wu, Haofan Yin, Cuncan Deng, and Ping Jiang. 2026. Integrative single-cell atlas unveils heterogeneity and prognostic value of cancer-associated fibroblasts in gastric cancer. Frontiers in Oncology 15 (2025), 1559489. Published online 9 January 2026. DOI: https://doi.org/10.3389/fonc.2025.1559489.

[53] Raghu Kalluri. 2016. The biology and function of fibroblasts in cancer. Nature Reviews Cancer 16, 9 (2016), 582–598.

[54] Luyao Kang, Zuchen Yang, Yanna Ding, Ying Wu, Caixia Ma, Yaping Wang, Canyu Li, Bilan Li, and Gaili Ji. 2026. Machine learning-based identification of an oxidative phosphorylation signature for prognosis, immune infiltration, and drug sensitivity in ovarian cancer. Frontiers in Immunology 17 (2026), 1724930. DOI: https://doi.org/10.3389/fimmu.2026.1724930.

[55] Wanyi Kou, Ruixin Guo, Yifan Zhang, Chensi Xu, Wenqi Sha, Yijie Chen, et al. 2026. An Eight-Gene Metabolic Prognostic Signature in Head and Neck Squamous Cell Carcinoma: Cross-Cohort Evaluation, Single-Cell Analysis, and Preliminary Functional Evaluation of PYGL and G6PD. Journal of Cancer 17, 11 (2026), 1895–1914. DOI: https://doi.org/10.7150/jca.134402.

[56] Julian Kreis, Bogac Aybey, Felix Geist, Benedikt Brors, and Eike Staub. 2024. Stromal Signals Dominate Gene Expression Signature Scores That Aim to Describe Cancer Cell–intrinsic Stemness or Mesenchymality Characteristics. Cancer Research Communications 4, 2 (2024), 516–529.

[57] Jian Li, Hong Pan, Yangyang Wang, Haixin Chen, Zhaopeng Song, Zheng Wang, and Jinxing Li. 2025. Construction of an Extracellular Matrix–Related Risk Model to Analyze the Correlation Between Glioblastoma and Tumor Immunity. BioMed Research International 2025, 1 (2025), 2004975. DOI: https://doi.org/10.1155/bmri/2004975.

[58] Mengtong Li, Jiayi Liu, Zichen Liu, Xia Liu, and Peng Lun. 2026. A Propionate Metabolism-Based Gene Signature Reveals Immunogenomic and Transcriptomic Determinants of Prognosis in Glioblastoma Through Multiomics Integration. Human Mutation 2026, 1 (2026), 6998123. DOI: https://doi.org/10.1155/humu/6998123.

[59] Quan Li, Pan Zhang, Huixiao Hu, Hang Huang, Dong Pan, Guangyun Mao, and Burong Hu. 2022. The DDR-related gene signature with cell cycle checkpoint function predicts prognosis, immune activity, and chemoradiotherapy response in lung adenocarcinoma. Respiratory Research 23, 1 (2022), 190.

[60] Tianhang Li, Ning Jiang, Yuhao Bai, Tianyao Liu, Zihan Zhao, Xinyan Xu, et al. 2023. Prediction of immune infiltration and prognosis for patients with urothelial bladder cancer based on the DNA damage repair-related genes signature. Heliyon 9, 3 (2023), e13661.

[61] Weifei Liang, Shi Zhang, Yuyang Zhang, Donglin Sun, Fang Wang, Hong Lin, and Yunhong Tian. 2026. A mitochondrial function-based prognostic model for hepatocellular carcinoma uncovers MRPS15 as a key driver of tumor progression through oxidative phosphorylation. Translational Cancer Research 15, 6 (2026), Article 496. DOI: https://doi.org/10.21037/tcr-2026-0426.

[62] Wanzun Lin, Shihong Wu, Xiaochuan Chen, Yuling Ye, Youliang Weng, Yuhui Pan, Zhangjie Chen, Long Chen, Xianxin Qiu, and Sufang Qiu. 2020. Characterization of Hypoxia Signature to Evaluate the Tumor Immune Microenvironment and Predict Prognosis in Glioma Groups. Frontiers in Oncology 10 (2020), 796.

[63] Zhuo Lin, Qian Xu, Dan Miao, and Fujun Yu. 2021. An Inflammatory ResponseRelated Gene Signature Can Impact the Immune Status and Predict the Prognosis of Hepatocellular Carcinoma. Frontiers in Oncology 11 (2021), 644416.

[64] Jianfang Liu, Tara Lichtenberg, Katherine A. Hoadley, Laila M. Poisson, Alexander J. Lazar, Andrew D. Cherniack, et al. 2018. An Integrated TCGA Pan-Cancer Clinical Data Resource to Drive High-Quality Survival Outcome Analytics. Cell 173, 2 (2018), 400–416.e11.

[65] Yongpan Lu, Sen Wang, Tingting Chi, Yuli Zhao, Huimin Guo, Haizheng Wang, and Li Feng. 2023. DNA damage repair-related gene signature for identifying the immune status and predicting the prognosis of hepatocellular carcinoma. Scientific Reports 13, 1 (2023), 18978.

[66] Chao Ma, Huan Luo, Jing Cao, Xiangyu Zheng, Jinjun Zhang, Yanmin Zhang, and Zongqiang Fu. 2020. Identification of a Novel Tumor Microenvironment–Associated Eight-Gene Signature for Prognosis Prediction in Lung Adenocarcinoma. Frontiers in Molecular Biosciences 7 (2020), 571641.

[67] Yihao Mao, Qingyang Feng, Peng Zheng, Liangliang Yang, Tianyu Liu, Yuqiu Xu, et al. 2018. Low tumor purity is associated with poor prognosis, heavy mutation burden, and intense immune phenotype in colon cancer. Cancer Management and Research Volume 10 (2018), 3569–3577.

[68] L M McShane, D G Altman, W Sauerbrei, S E Taube, M Gion, and G M Clark. 2005. REporting recommendations for tumour MARKer prognostic studies (REMARK). British Journal of Cancer 93, 4 (2005), 387–391.

[69] Stefan Michiels, Serge Koscielny, and Catherine Hill. 2005. Prediction of cancer outcome with microarrays: a multiple random validation strategy. The Lancet 365, 9458 (2005), 488–492.

[70] Richard A Moffitt, Raoud Marayati, Elizabeth L Flate, Keith E Volmar, S Gabriela Herrera Loeza, Katherine A Hoadley, et al. 2015. Virtual microdissection identifies distinct tumorand stroma-specific subtypes of pancreatic ductal adenocarcinoma. Nature Genetics 47, 10 (2015), 1168–1178.

[71] Jeffrey S. Morris and Scott Kopetz. 2016. Tumor Microenvironment in Gene Signatures: Critical Biology or Confounding Noise? Clinical Cancer Research 22, 16 (2016), 3989–3991.

[72] Aaron M Newman, Chih Long Liu, Michael R Green, Andrew J Gentles, Weiguo Feng, Yue Xu, Chuong D Hoang, Maximilian Diehn, and Ash A Alizadeh. 2015. Robust enumeration of cell subsets from tissue expression profiles. Nature Methods 12, 5 (2015), 453–457.

[73] Prasad Patil, Pierre-Olivier Bachant-Winner, Benjamin Haibe-Kains, and Jeffrey T. Leek. 2015. Test set bias affects reproducibility of gene signatures. Bioinformatics 31, 14 (2015), 2318–2323.

[74] Chen Qian, Wu Xiufu, Tang Jianxun, Chen Zihao, Shi Wenjie, Tang Jingfeng, Ulf D. Kahlert, and Du Renfei. 2022. A Novel Extracellular Matrix Gene-Based Prognostic Model to Predict Overall Survive in Patients With Glioblastoma. Frontiers in Genetics 13 (2022), 851427.

[75] Egor Revkov, Tanmay Kulshrestha, Ken Wing-Kin Sung, and Anders Jacobsen Skanderup. 2023. PUREE: accurate pan-cancer tumor purity estimation from gene expression data. Communications Biology 6, 1 (2023), 394.

[76] Je-Keun Rhee, Yu Chae Jung, Kyu Ryung Kim, Jinseon Yoo, Jeeyoon Kim, Yong-Jae Lee, Yoon Ho Ko, Han Hong Lee, Byoung Chul Cho, and Tae-Min Kim. 2018. Impact of Tumor Purity on Immune Gene Expression and Clustering Analyses across Multiple Cancer Types. Cancer Immunology Research 6, 1 (2018), 87–97.

[77] Enrique F. Schisterman, Stephen R. Cole, and Robert W. Platt. 2009. Overadjustment Bias and Unnecessary Adjustment in Epidemiologic Studies. Epidemiology 20, 4 (2009), 488–495.

[78] Yangyang She, Xiangbo Kong, Yaping Ge, Ping Yin, Zhiyong Liu, Jieyu Chen, Feng Gao, and Silian Fang. 2020. Immune-related gene signature for predicting the prognosis of head and neck squamous cell carcinoma. Cancer Cell International 20, 1 (2020), 22.

[79] Fengjuan Shi, Tongning Deng, Jian Mo, Huiru Wang, and Jianxun Lu. 2021. An Immune-Related Gene-Based Signature as Prognostic Tool in Ovarian Serous Cystadenocarcinoma. International Journal of General Medicine Volume 14 (2021), 4095–4104.

[80] Joan C. Smith and Jason M. Sheltzer. 2022. Genome-wide identification and analysis of prognostic features in human cancers. Cell Reports 38, 13 (2022),

110569.

[81] Gregor Sturm, Francesca Finotello, Florent Petitprez, Jitao David Zhang, Jan Baumbach, Wolf H Fridman, Markus List, and Tatsiana Aneichyk. 2019. Comprehensive evaluation of transcriptome-based cell-type quantification methods for immuno-oncology. Bioinformatics 35, 14 (2019), i436–i445.

[82] Keran Sun and Keqi Jia. 2026. Development and Validation of a Pan-Cancer Stromal Activity Score for Predicting Prognosis and Immunotherapy Response. medRxiv preprint (2026). DOI: https://doi.org/10.64898/2026.07.21.26358625.

[83] Kai Sun, Ke-run Wang, Song Wen, Juan-juan Hong, Yu-lang Fei, Qing-hua Pan, and Fang-fang Xie. 2025. Identification and experimental verification of necroptosis-related prognostic gene signature and characterization of tumor immune infiltration in lung squamous cell carcinoma. PeerJ 13 (2025), e20260. DOI: https://doi.org/10.7717/peerj.20260.

[84] Xianchao Sun, Zhen Zhou, Ying Zhang, Jinyou Wang, Xiaofeng Zhao, Liang Jin, et al. 2021. Identification and validation of a hypoxia-related prognostic and immune microenvironment signature in bladder cancer. Cancer Cell International 21, 1 (2021), 251.

[85] H. Tang, S. Wang, G. Xiao, J. Schiller, V. Papadimitrakopoulou, J. Minna, I.I. Wistuba, and Y. Xie. 2017. Comprehensive evaluation of published gene expression prognostic signatures for biomarker-based lung cancer clinical studies. Annals of Oncology 28, 4 (2017), 733–740.

[86] Vésteinn Thorsson, David L. Gibbs, Scott D. Brown, Denise Wolf, Dante S. Bortone, Tai-Hsien Ou Yang, et al. 2018. The Immune Landscape of Cancer. Immunity 48, 4 (2018), 812–830.e14.

[87] Zhouting Tuo, Yuan Lin, Ying Zhang, Liang Gao, Dexin Yu, Jiani Wang, et al. 2024. Prognostic significance and immune landscape of a cell cycle progressionrelated risk model in bladder cancer. Discover Oncology 15, 1 (2024), 160.

[88] David Venet, Jacques E. Dumont, and Vincent Detours. 2011. Most Random Gene Expression Signatures Are Significantly Associated with Breast Cancer Outcome. PLoS Computational Biology 7, 10 (2011), e1002240.

[89] Erik von Elm, Douglas G Altman, Matthias Egger, Stuart J Pocock, Peter C Gøtzsche, and Jan P Vandenbroucke. 2007. The Strengthening the Reporting of Observational Studies in Epidemiology (STROBE) statement: guidelines for reporting observational studies. The Lancet 370, 9596 (2007), 1453–1457.

[90] Huan Wang, Luhui Li, Dingyuan Tu, Ping Shen, Zheyao Song, Mengjiao An, Xudong Li, Qi Ji, Peng Chen, and Rongjun Cui. 2026. Bulk and single-cell RNA sequencing data identified HMGB3 of chromatin regulators as a breast cancer biomarker associated with the cell cycle. Frontiers in Oncology 16 (2026), 1835558. DOI: https://doi.org/10.3389/fonc.2026.1835558.

[91] D. Westreich and S. Greenland. 2013. The Table 2 Fallacy: Presenting and Interpreting Confounder and Modifier Coefficients. American Journal of Epidemiology 177, 4 (2013), 292–298.

[92] Michael L. Whitfield, Lacy K. George, Gavin D. Grant, and Charles M. Perou. 2006. Common markers of proliferation. Nature Reviews Cancer 6, 2 (2006), 99–106.

[93] Chengting Wu, Yuanqin Du, Juhong Jia, Xinyuan Chen, Longda Wu, Yaran Zhao, et al. 2026. A novel hypoxia-related signature for predicting prognosis, immune characteristics, and therapeutic response in hepatocellular carcinoma. Discover Oncology 17 (2026), Article 1168. DOI: https://doi.org/10.1007/s12672-026-05691-w.

[94] Zi-Zheng Wu, Yuan-Jun Wei, Tong Li, Jie Zheng, Yin-Feng Liu, and Meng Han. 2024. Identification and validation of a new prognostic signature based on cancer-associated fibroblast-driven genes in breast cancer. World Journal of Clinical Cases 12, 4 (2024), 700–720.

[95] Peng Xing, Zhengming Jiang, and Yang Liu. 2022. Construction and validation of a gene signature related to bladder urothelial carcinoma based on immune gene analysis. BMC Cancer 22, 1 (2022), 926.

[96] Hui Xu, Meng Li, Wen-lan Qiao, and Tian Hua. 2026. Establishment of a Prognostic Necroptosis-Related lncRNA Signature in Ovarian Cancer. Combinatorial Chemistry & High Throughput Screening 29, 4 (2026), 577–594. DOI: https://doi.org/10.2174/0113862073339602241028095015.

[97] Nan Xu, Taojing Zhang, Weiwei Sun, Chenxiao Ye, and Huamiao Zhou. 2025. Identification of an extracellular matrix signature for predicting prognosis and sensitivity to therapy of patients with gastric cancer. Scientific Reports 15, 1 (2025), 7464. DOI: https://doi.org/10.1038/s41598-025-88376-8.

[98] Biao Yang, Ren Li, and Hubin Duan. 2026. Associations between migrasomerelated genes and long non-coding rnas in glioma and their prognostic relevance to the tumor microenvironment. IBRO Neuroscience Reports 21 (2026), 279–290. DOI: https://doi.org/10.1016/j.ibneur.2026.06.013.

[99] Jian Yang, Zhike Chen, Zetian Gong, Qifan Li, Hao Ding, Yuan Cui, et al. 2022. Immune Landscape and Classification in Lung Adenocarcinoma Based on a Novel Cell Cycle Checkpoints Related Signature for Predicting Prognosis and Therapeutic Response. Frontiers in Genetics 13 (2022), 908104.

[100] Zhenbang Ye, Ning Huang, Yongliang Fu, Rongle Tian, Liming Wang, and Wenting Huang. 2024. Tumor purity-related genes for predicting the prognosis and drug sensitivity of DLBCL patients. eLife 13 (2024), RP92841.

[101] Kosuke Yoshihara, Maria Shahmoradgoli, Emmanuel Martínez, Rahulsimham Vegesna, Hoon Kim, Wandaliz Torres-Garcia, et al. 2013. Inferring tumour purity and stromal and immune cell admixture from expression data. Nature Communications 4, 1 (2013), 2612.

[102] Ziye Yu, Huan Yang, Kun Song, Pengfei Fu, Jingjing Shen, Ming Xu, and Hongzhi Xu. 2022. Construction of an immune-related gene signature for the prognosis and diagnosis of glioblastoma multiforme. Frontiers in Oncology 12 (2022), 938679.

[103] Jiaoyang Zhan, Shuang Wu, Xu Zhao, and Jingjing Jing. 2021. A Novel DNA Damage Repair-Related Gene Signature for Predicting Glioma Prognosis. International Journal of General Medicine Volume 14 (2021), 10083–10101.

[104] Anran Zhang, Jinpo Yang, Chao Ma, Feng Li, and Huan Luo. 2021. Development and Validation of a Robust Ferroptosis-Related Prognostic Signature in Lung Adenocarcinoma. Frontiers in Cell and Developmental Biology 9 (2021), 616271.

[105] Chuanbao Zhang, Wen Cheng, Xiufang Ren, Zheng Wang, Xing Liu, Guanzhang Li, Sheng Han, Tao Jiang, and Anhua Wu. 2017. Tumor Purity as an Underlying Key Factor in Glioma. Clinical Cancer Research 23, 20 (2017), 6279–6291.

[106] Feng Zhang, Jian Fu, Xuxu Cui, Xutong Gao, and Yanxia Kang. 2026. Development and internal validation of a six-gene prognostic model based on galactose metabolism for overall survival in lung adenocarcinoma. Translational Cancer Research 15, 8 (2026), Article 586. DOI: https://doi.org/10.21037/tcr-2026-0696.

[107] Lian-Qun Zhang, Sheng-Li Zhou, Jun-Kuo Li, Pei-Nan Chen, Xue-Ke Zhao, LiDong Wang, Xiu-Ling Li, and Fu-You Zhou. 2022. Identification of a seven-cell cycle signature predicting overall survival for gastric cancer. Aging 14, 9 (2022), 3989–3999.

[108] Wenqi Zhang, Xiangran Gu, Zhengrong Yuan, and Haiyan Zhang. 2026. Disulfidptosis-related genes and long non-coding RNAs define a prognostic model for liver cancer. Translational Cancer Research 15, 9 (2026), Article 676. DOI: https://doi.org/10.21037/tcr-2026-0908.

[109] Yang Zhang, Shuanggong Liu, Guangxu Song, Kewen Wang, Zhi Zhou, Yueying Xiao, and Dongjin Wu. 2026. Development and validation of a phospholipid metabolism-associated lncRNA model for prognostic stratification and therapeutic guidance in HNSCC. World Journal of Surgical Oncology 24, 1 (2026), 183. DOI: https://doi.org/10.1186/s12957-026-04299-2.

[110] Zhaoqi Zhang, Ying Wang, Wei Yin, Qingyang Lei, Yuqiao Fu, Yingzi Liang, Ruilei Li, and Ke Li. 2025. Identification and validation of prognostic genes and prognostic models associated with cutaneous melanoma and integrative stress response. Frontiers in Immunology 16 (2025), 1689103. DOI: https://doi.org/10.3389/fimmu.2025.1689103.

[111] Ziran Zhang, Xingxia Yang, Jie Tang, Lifen Cai, and Jingying Feng. 2026. A prognostic risk model based on programmed cell death genes for breast cancer and its potential clinical application. Medicine 105, 30 (2026), e49607. DOI: https://doi.org/10.1097/MD.0000000000049607.

[112] Lei Zhao, Zhi-Cai Li, Zhou-You Tang, Yu-Tong Yuan, and Shan Zhu. 2026. A tryptophan metabolism-related gene signature predicts prognosis and immune features in cutaneous melanoma. Frontiers in Immunology 17 (2026), 1806319. DOI: https://doi.org/10.3389/fimmu.2026.1806319.

[113] Yan Zhao, Xu Xu, Yue Wang, Lin D. Wu, Rui L. Luo, and Ren P. Xia. 2023. Tumor purity–associated genes influence hepatocellular carcinoma prognosis and tumor microenvironment. Frontiers in Oncology 13 (2023), 1197898.

[114] Xiaobin Zhou, Hui Liang, and Qinhong Huang. 2026. Peroxisomal fatty acid oxidation-related signature for predicting prognosis and therapeutic response in low-grade glioma. Frontiers in Oncology 16 (2026), 1897651. DOI: https://doi.org/10.3389/fonc.2026.1897651.

[115] Zijian Zhou, Yuan Xiang, Annan Wu, Yiwei Zhang, Lei Xie, Yajie Zhou, Wenxiong Zhang, and Queling Liu. 2025. Identification and external validation of a prognostic signature based on hypoxia–glycolysis-related genes for kidney renal clear cell carcinoma. Open Medicine 20, 1 (2025), 20251305. DOI: https://doi.org/10.1515/med-2025-1305.